HHS Public Access

Author manuscript

J Vasc Surg. Author manuscript; available in PMC 2020 April 19.

Published in final edited form as:

J Vasc Surg. 2018 June ; 67(6): 1908–1920.e1. doi:10.1016/j.jvs.2017.04.070.

Recruitment and therapeutic application of macrophages in skeletal muscles after hind limb ischemia

Pei-Ling Hsieh, PhD[a], **Viktoriya Rybalko, PhD**[b], **Aaron B. Baker, PhD**[b], **Laura J. Suggs, PhD**[b], **Roger P. Farrar, PhD**[a]

[a]Department of Kinesiology, The University of Texas at Austin.

[b]Department of Biomedical Engineering, The University of Texas at Austin.

Abstract

Objective: Peripheral arterial disease can cause not only ischemia but also skeletal muscle damage. It has been known that macrophages (MPs) play an important role in coordinating muscle repair; however, phenotype transition of monocyte-MP in ischemic muscle has not been well defined. Hence, the purpose of this study was to examine the temporal recruitment of MPs and to explore their therapeutic effect on ischemic muscle regeneration.

Methods: Unilateral femoral artery excision was performed on C57BL/6 mice. Myeloid cells were isolated from the ischemic muscles, characterized using flow cytometry. Bone marrow-derived MPs were injected (2×10^6 cells) into the ischemic gastrocnemius muscle 24 hours after injury. Blood flow recovery was measured using laser speckle imaging. Functional outcome was evaluated by assessing the contractile force of ischemic muscles. Histologic analysis included quantification of myofiber size, collagen deposition, number of inflammatory and MyoD-expressing cells, and capillary density.

Results: Neutrophils and inflammatory monocytes-MPs were present at day 1 after injury. The mature MPs then remained elevated as the dominant population from day 5 to day 21 with the observation of regenerating fibers. Functional measurements revealed that the force production was significantly enhanced after treatment with proinflammatory M1 MPs (94.9% vs 77.9%; $P < .05$), and this was consistent with increased myofiber size, capillary-fiber ratio, and perfusion (78.6% vs 39.9%; $P < .05$). Moreover, the percentage of MyoD-expressing nuclei was significantly higher at day 4, indicating that M1 MPs may hasten muscle repair. Whereas early delivery of anti-

Correspondence: Roger P. Farrar, PhD, Department of Kinesiology, The University of Texas at Austin, 2109 San Jacinto Blvd, D3700, Austin, TX 78712 (rfarrar@austin.utexas.edu).

AUTHOR CONTRIBUTIONS

Conception and design: PH, VR, RF

Analysis and interpretation: PH, VR, AB, LS Data collection: PH, VR

Writing the article: PH

Critical revision of the article: VR, AB, LS, RF Final approval of the article: PH, VR, AB, LS, RF

Statistical analysis: PH, AB

Obtained funding: LS, RF

Overall responsibility: PH

Author conflict of interest: none.

Additional material for this article may be found online at www.jvascsurg.org.

The editors and reviewers of this article have no relevant financial relationships to disclose per the JVS policy that requires reviewers to decline review of any manuscript for which they may have a conflict of interest.

inflammatory M2 MPs improved myofiber size, this was accompanied by persistent fibrosis suggesting ongoing tissue remodeling, and lower force production was observed.

Conclusions: We demonstrated the dynamics of myeloid cells in skeletal muscle after ischemic insult, and the administration of exogenous M1 MPs in a temporally coordinated manner successfully improved angiogenesis and skeletal muscle regeneration. Our results suggested that cell therapy using MPs may be a promising adjunctive therapeutic approach for peripheral arterial disease.

Clinical Relevance: Many patients with peripheral arterial disease have reduced muscle size, reduced strength, and impaired walking ability, which greatly affect their quality of life. Unfortunately, effective therapeutic options for patients with advanced cardiovascular disease are limited. Therefore, we aimed to examine the efficacy of intramuscular administration of macrophages on angiogenesis as well as muscle recovery. Results from this study can be used as preclinical knowledge to guide the development of cell therapy and to enhance ischemic muscle regeneration.

In the United States, it is estimated that more than eight million individuals suffer from peripheral arterial disease (PAD),[1] which is related to increased cardiovascular disease[2] and functional impairment.[3] Several studies have shown that PAD has a direct adverse effect on calf muscles through progressive ischemia, resulting in muscle damage and reduced strength.[4] Reduction in muscle size and strength is associated with accelerated functional decline and greater impairment.[4] As such, in addition to restoration of the blood supply, skeletal muscle regeneration and recovery of contractile force are crucial components that need to be considered in developing treatments for PAD.

Injury to skeletal muscle is normally followed by inflammatory cell infiltration and subsequent tissue repair.[5] Multiple myeloid cell populations regulate the regenerative process, and transition of myeloid cell phenotypes often coincides with the changes of myogenic transcription factors related to proliferation and differentiation of myogenic progenitor cells (see review[6]). Aside from their roles in immune surveillance and immune defense, macrophages (MPs) play important roles in angiogenesis[7,8] and tissue remodeling.[7] After injury, the recruited MPs facilitate wound healing through phagocytosis of injured cells[5] as well as by modulation of muscle progenitor cells[9] and release of insulin-like growth factor 1 (IGF-1).[10] Whereas the in vivo transition from M1 to M2 MP phenotype is a continuum, in vitro activation of M0 to inflammatory MPs (M1 MPs) can be achieved through treatment with lipopolysaccharide (LPS) and interferon-γ (IFN-γ). M1 MPs are associated with the production of proinflammatory cytokines and reactive oxygen species. In the presence of interleukin 4 (IL-4) and IL-13, MPs become alternatively activated (M2 MPs) and are associated with anti-inflammatory cytokine production and reduced major histocompatibility complex class II expression (see review[11]).

The accumulation of perivascular MPs after femoral artery excision (FAE) has been examined.[12] However, little is known about the dynamics of the myeloid cell accumulation in ischemic muscles. In addition, although a number of experiments suggested the potential of using MP therapy to enhance the restoration of blood supply[13–15] and various clinical studies showed improved perfusion after cell therapy (see review[16]), its effect on muscle

repair after FAE remains to be elucidated. In a previous study,[10] we performed intramuscular injection of $CD11b^{+}Ly\text{-}6C^{lo}F4/80^{hi}$ cells isolated from muscles after ischemia-reperfusion (I/R) injury and found significant improvement of muscle size and force. Furthermore, our recent data revealed that in vitro polarized M1 MPs significantly improved muscle repair after I/R injury by decreasing fibrotic tissue deposition and increasing whole muscle IGF-1 expression.[17] Therefore, we hypothesized that intramuscular delivery of MPs could improve the perfusion and enhance muscle regeneration in the FAE model.

In this study, we investigated the temporal kinetics of myeloid cell accumulation or how recruitment coincides with the regenerative events in the ischemic muscles. These results provide important information in terms of determining the optimal time point for cell transplantation. Moreover, intramuscular administration of exogenous in vitro polarized M1 MPs restored muscle perfusion, increased myofiber size, decreased fibrosis, and improved muscle contractile force. There were a higher proportion of $MyoD^{+}$ nuclei at day 4 and fewer infiltrating cells at day 21, indicating the accelerated muscle regeneration and resolution of inflammation after administration of M1 MPs. Our findings support the idea of using polarized MPs as a treatment modality to improve angiogenesis and muscle regeneration for PAD, especially in a temporally coordinated manner.

METHODS

All experimental procedures and protocols were approved in accordance with the guidelines set by The University of Texas at Austin Institutional Animal Care and Use Committee.

Murine unilateral hind limb ischemia injury.

Unilateral FAE was performed on female C57BL/6 mice (Jackson Laboratories, Bar Harbor, Me) under 2% isoflurane inhalation anesthesia. The detailed surgical procedures are described in the Supplementary Methods (online only). Animals were allowed to recover with a heating pad until ambulatory. Mice were then returned to their cages and housed with ad libitum access to food and water and maintained on a 12-hour light-dark cycle.

Laser speckle imaging of blood flow.—Laser speckle imaging is a validated method to visualize tissue blood perfusion.[18] The feet of the mice were imaged at 1 day and 21 days after FAE to confirm the ischemia and to examine the effects of treatment, respectively. Blood flow was examined as previously described.[19] Briefly, a diode laser (785-nm, 50-mW; Thor Labs, Newton, NJ) was applied on the footpad of a mouse under anesthesia. The speckle images of blood perfusion were captured by a Basler 1920 × 1080 monochrome CCD with a zoom lens (Zoom7000; Navitar, Rochester, NY) mounted on a microscope boom stand and quantified using MATLAB (MathWorks, Natick, Mass) and Meta-Morph (Molecular Devices, Sunnyvale, Calif). Relative perfusion was expressed as a ratio of left (ischemic) to right (uninjured) limb.

Functional measurements of muscle contractile force.

As previously described,[10] mice were anesthetized using 2% isoflurane and maintained at 37°C using a heat lamp. Triceps surae muscles were surgically isolated from other tissue,

and the distal femoral condyle was immobilized to a stainless steel platform. The detailed surgical procedures and settings are described in the Supplementary Methods (online only). At optimal length, the muscle was stimulated at 150 Hz to elicit the peak tetanic tension with 2 minutes of rest between each contraction. Data were stored and analyzed using LabView software (National Instruments, Austin, Tex).

Histologic preparation and analysis.

Frozen, optimal cutting temperature compound-embedded muscle samples were sectioned into 10-μm sections using a cryostat (Leica CM1900; Leica Microsystems Inc, Buffalo Grove, Ill). Cryosections were stained with hematoxylin and eosin for gross morphologic examination or Masson trichrome (Polyscience, Warrington, Pa) for collagen deposition as previously described.[20] To identify endothelial cells and inflammatory cells, the sections were stained with anti-CD31 antibody or anti-CD45 antibody. Anti-MyoD antibody was applied to the sections to examine the myogenesis. Regenerating fibers were identified by characteristic centrally located nuclei. Capillary-fiber ratio was determined from the number of $CD31^+$ cells per muscle fiber. Immune cell infiltrate was expressed as the number of $CD45^+$ cells per field of view. $MyoD^+$ cells were quantified as a percentage of total nuclei from the tile scanned image (2 × 2 tiles; 10% overlap). Myofiber cross-sectional area and collagen accumulation were quantified using ImageJ software (National Institutes of Health, Bethesda, Md).

Flow cytometry analysis of myeloid cells in ischemic muscles.

Total cells present in muscle after FAE injury were isolated by enzymatic digest as previously described.[10] Cells were washed with 1% bovine serum albumin in phosphate-buffered saline (PBS); blocked with 2% bovine serum albumin in PBS with addition of Fcγ-block (eBioscience, San Diego, Calif); and stained with either a cocktail containing phycoerythrin-conjugated anti-CD11b (BD Biosciences, Franklin Lakes, NJ), peridinin-chlorophyll-conjugated anti-Gr1 (BioLegend, San Diego, Calif), fluorescein isothiocyanate-conjugated anti-Ly6C (BioLegend), and allophycocyanin-conjugated anti-F4/80 (BioLegend) or a cocktail of the corresponding isotype controls. Samples were run on the BD Fortessa Flow Cytometer (BD Biosciences) at The University of Texas at Austin Institute of Cell and Molecular Biology core facility with the forward scatter settings gated to exclude red blood cell-sized cells. Data were analyzed using FlowJo software (FlowJo, LLC, Ashland, Ore).

Isolation of bone marrow (BM) and activation of MPs.

BM-derived MPs were isolated and polarized in vitro as previously described.[17] Cells were cultured in Dulbecco modified Eagle medium supplemented with 10% fetal bovine serum, 1% antibiotic-antimycotic, and 10 ng/mL MP colony-stimulating factor at 1.5 to 2×10^6 cells/mL in six-well plates for 5 days. Unpolarized MPs were designated M0. For MP polarization, cells were treated with 10 ng/mL type I IFN-γ and LPS or 10 ng/mL IL-4 and IL-13 to obtain M1 and M2 MPs, respectively. After 42 hours of cytokine exposure, MPs were harvested for RNA isolation or MP cell therapy.

RNA isolation and real-time polymerase chain reaction (PCR).

Total RNA was extracted from BM-derived MPs using Direct-zol RNA MiniPrep Kit (Zymo Research, Irvine, Calif) and reverse transcribed using the SuperScript III Kit (Invitrogen, Carlsbad, Calif) according to manufacturers' instructions. Real-time PCR analysis was performed on the iCycler iQ5 (Bio-Rad, Hercules, Calif) using corresponding primers (Table) and SYBR Green Master Mix (Bio-Rad). Relative gene expression was determined using the ΔΔCt method with β-actin as the loading controls for isolated cells.

MP cell therapy.

BM-derived MPs were treated with trypsin for 2 minutes at 37°C to lift cells off the tissue culture plates. Cells were washed three times with PBS (pH 7.4), counted using a hemocytometer, and resus-pended at 2×10^6 cells in 60 μL of PBS. Injection of M0, M1, and M2 MPs or PBS vehicle into ischemic gastrocnemius muscles was performed 24 hours after FAE, and muscles were collected for histologic analysis of regeneration and fibrosis.

Statistical analysis.

All values are presented as means ± standard error of the mean. Comparisons between groups were analyzed using one-way analysis of variance followed by Tukey honest significant difference or Dunnett post hoc test ($P < .05$ was considered statistically significant).

RESULTS

FAE results in persistent muscle force reduction and collagen deposition.

After ischemic insult, we excised the muscles at day 21 for histologic analysis. Hematoxylin and eosin images showed that muscle myofibers underwent degeneration by day 3 after FAE with infiltrating inflammatory cells between myofibers, which was consistent with previous studies.[21,22] The regenerating fibers, characterized by centrally located nuclei, appeared on day 5 (Fig 1, *A*). The collagen deposition became obvious at later time points (Fig 1, *B*). By seven days, the average cross-sectional area indicated that the myofiber size was significantly smaller relative to the contralateral control. The decreased myofiber size persisted until at least day 28 (Fig 1, *C*). Several studies have shown the gradual restoration of perfusion in the first 2 weeks after FAE.[23,24] Nevertheless, insufficient blood supply or limb ischemia during exercise seemed to evoke another wave of cell infiltrate at 21 days after FAE (Fig 1, *A*) because mice have high levels of spontaneous activity and females have impaired recovery of blood flow.[24] This phenomenon of recurrent cell infiltrate may be related to increased oxidative stress and endothelial dysfunction.[25,26] The percentage of the muscle area occupied by the regenerating fibers increased on days 21 and 28 (Fig 1, *D*). Collectively, these results showed that there was an ongoing degenerative-regenerative sequence in the presence of compromised blood supply to the muscle. It is well established that residual inflammation in the course of tissue regeneration may adversely affect tissue repair by facilitating excessive connective tissue deposition, also known as fibrosis.[27] We evaluated the extent of fibrotic tissue deposition in the recovering muscle by performing Masson trichrome staining. Our data showed significant collagen deposition at 21 and 28

days after FAE (Fig 1, *B* and E). Functional performance of regenerating muscle was analyzed using a muscle lever system. By day 14, the normalized force was significantly lower compared with the contralateral side (Fig 1, *F*). Together, these results suggested that the increased collagen accumulation and decreased myofiber size may contribute to the reduced muscle force production after FAE injury.

MP profiles and phenotypes after murine hind limb ischemia injury.

To examine the kinetics of myeloid cells in the ischemic muscles, we performed flow cytometric analysis of freshly isolated cells from FAE-injured muscles at various time points after injury. We used a specific antibody cocktail against CD11b to identify myeloid cells, GR-1, and Ly-6C to differentiate between neutrophils and inflammatory monocytes (MOs)-MPs as well as F4/80 to stain for mature MPs. Because Ly-6C is a surface marker found on inflammatory MOs/MPs and neutrophils, we defined the Ly-6C^{hi}F4/80^{lo} as M1 MPs and Ly-6C^{lo}F4/80^{hi} as M2 MPs in this study.

Consistent with our previous report on cell immunophenotyping after tourniquet I/R injury, [10] there was an acute temporal transition of myeloid cells from primarily Ly-6C^{hi}F4/80^{lo} toward Ly-6C^{lo}F4/80^{hi} in post-FAE muscles (Fig 2, *A*), indicating that the switch from an inflammatory MO/MP (M0/M1) to a mature MP (M2) phenotype occurred between day 1 and day 3 after injury. In agreement with the total cell number and histologic findings that inflammatory cell influx occurred on day 3 (Figs 1, *A* and 2, *B*), the CD11b^{+} and Ly-6C^{+}F4/80$^{lo/-}$ cells reached the peak number at day 3 after FAE (Fig 2, *C* and D), as did the mature MPs (Fig 2, *E*). As mentioned before, even though there was a decline in total cell number, it increased again on day 21 compared with uninjured muscle ($P = .006$ using Student *t*-test). This may be an indication of continuing muscle damage after the sustained reduction in blood supply. Furthermore, we performed a relative quantification of MO/MP percentages among total CD11b^{+} cells (Fig 2, *F*). At day 1, most of the myeloid cells were neutrophils (GR-1^{+}Ly-6C^{-}F4/80^{-}; 37.2%) and inflammatory MOs/MPs (GR-1^{-}Ly-6C^{+}F4/80$^{lo/-}$; 25.7%), and the remaining were mature MPs and triple-negative cells. Shortly after neutrophil invasion, the inflammatory MOs/MPs subsequently switched into mature MPs. At day 3, inflammatory MOs/MPs (29.7%) and mature MPs (GR-1^{-}Ly-6C^{-}F4/80^{+}; 38.6%) were the dominant cell phenotypes. Mature MPs then became the majority (54.9%) at day 5 and remained as the most prevalent population in day 14 and day 21 muscles, coinciding with the observation of regenerating fibers in our histologic results.

Gene expression of the in vitro polarized BM-derived MPs.

Arnold et al[9] have sorted cells after muscle injury and correlated gene expression to surface markers. They showed that Ly-6C^{+} MOs/MPs expressed higher IL-1β and tumor necrosis factor α (TNF-α) than Ly-6C^{-} MOs/MPs, and Ly-6C^{-} MOs/MPs expressed more transforming growth factor β1 [TGF-β1] and IL-10 than Ly-6C^{+} MOs/MPs.

Moreover, they demonstrated that LPS and IFN-γ treatment of human MPs induced TNF-α and IL-1β secretion, whereas IL-4 treatment induced TGF-β1 secretion. To confirm the MP polarization state and to examine the transcriptional profile in this study, we analyzed gene expression of the BM-derived MPs by real-time PCR after 42 hours of stimulation. LPS- and

IFN-γ-treated M1 MPs had upregulated the proinflammatory IL-1β and inducible nitric oxide synthase and decreased the anti-inflammatory peroxisome proliferator-activated receptor g gene expression compared with the unstimulated M0 MPs (Fig 3, *A* and B). Conversely, IL-4- and IL-13-treated M2 MPs had lower proinflammatory IL-1β expression and higher levels of anti-inflammatory Ym-1 in comparison to M0 MPs (Fig 3, *A* and B). These results verified that BM-derived MPs were successfully polarized to become M1 or M2 MPs characterized in the literature.[28–30]

M1 MP therapy restores perfusion and the number of endothelial cells in ischemic muscles.

In accordance with prior studies using laser Doppler imaging,[12,15] our laser speckle imaging results also showed a sustained reduction in blood supply in PBS- or M0 MP-treated groups at day 21 along with reduced capillary density (Fig 4, *A* and B). Intramuscular delivery of M1 MPs revealed significant improvement of perfusion compared with day 1 after FAE (Fig 4, *A* and C), indicating that in vitro polarized MP transplantation in the ischemic muscles could enhance blood flow recovery. Immunohistochemistry of CD31 staining showed that administration of M1 MPs significantly increased the capillary-fiber ratio compared with the PBS-treated group (Fig 4, *B* and D), consistent with the increased perfusion observed with laser speckle imaging. These results clearly demonstrated that early delivery of M1 MPs could effectively improve the ischemic condition by enhancing muscle perfusion.

Intramuscular M1 MP therapy improves muscle morphology and fibrosis.

Our previous study demonstrated that increasing numbers of M1 MPs early after I/R injury facilitate faster debris clearance and accelerated muscle repair.[17] To study whether increasing the amount of MPs in the ischemic muscles after FAE is beneficial, we injected PBS and M0, M1, or M2 MPs in the gastrocnemius muscles 24 hours after FAE. We conducted histologic analysis and found that the myofiber distribution gave evidence of significant reduction in myofiber size in the PBS-treated muscles compared with the contralateral control muscles (Fig 5, *A* and B). The M0 MP treatment group had a similar shift toward smaller myofiber diameters, whereas treatment with M1 and M2 MPs prevented this reduction. Delivery of M1 MPs increased the average myofiber size and significantly reduced the proportion of the smaller myofibers as well as collagen deposition (Fig 5, *C*–F), suggesting that there were more mature myofibers after treatment.

MP therapy improves functional recovery of ischemic muscles.

The deficit in muscle force production causes functional impairment in PAD patients,[4,31] and this phenomenon was recapitulated in our FAE model. Our results showed that although there was no difference in muscle mass among all groups (Fig 6, *A*), the ability of the M1 MP group to restore the tetanic tension was markedly better (85.9% of contralateral control) compared with the PBS-treated (76.2% of control; $P < .05$ compared with M1 MPs), M0 MP-treated (73.4% of control; $P < .05$ compared with M1 MPs), and M2 MP-treated (73.02% of control; $P < .05$ compared with M1 MPs) groups (Fig 6, *B*). M1 MP treatment also significantly enhanced recovery of muscle force normalized to mass (96.5% of contralateral control) at 21 days after FAE, whereas the strength of other groups remained impaired (Fig 6, *C*).

Early delivery of M1 MPs accelerates myogenesis and resolution of inflammation.

To evaluate the myogenesis after treatment, we stained the muscle with the early myogenic marker MyoD at day 4 after FAE (Fig 7). Our result showed that the percentage of MyoD-expressing nuclei was significantly increased in M1 MP-treated muscles (42.3%) compared with the PBS group (19.8%; Fig 7). Previously, we have shown the transplanted M1 MPs could promote a faster MP transition from M1- to M2-like phenotype in I/R injured muscles.[17] In this study, we further confirmed that the delivery of M1 MPs could hasten the regeneration processes of the ischemic muscles with the increased expression of MyoD at an early time point. In addition, we observed the decreased number of $CD45^+$ cells in M1 MP-treated muscles compared with other groups, indicating the reduced immune cell infiltrate at day 21 (Fig 8). Taken together, these findings suggested that M1 MP-treated muscles displayed a better recovery of skeletal muscle.

DISCUSSION

MPs are important for skeletal muscle regeneration not only through clearance of cellular debris but also by modulating satellite cell activation and tissue fibrosis during healing. Our results showed that there was pathologic fibrosis after ischemia along with increased M2 MPs (Fig 1, *E*), and this phenomenon may be associated with the MP-regulated fibro/adipogenic precursor cells (FAPs). Usually, the number of FAPs would return to pre-injury level at an early stage before they differentiate into fibroblasts. In this model, the elevated M2 MPs may lead to an increase in FAPs. It has been shown that TGF-β secreted by M2 MPs blocked TNF-α-induced apoptosis of FAPs and increased the expression of collagen in vivo.[32] In addition, Shireman et al[21] reported that both neutrophils and MPs were present in day 3 muscles after ischemic injury. Our work has added to these by using a flow cytometric study to analyze MP profiles over time after ischemia in association with muscle recovery. These results would provide valuable information for other investigators in deciding the timing of cell delivery.

A number of mechanisms may be responsible for the observed effects in this study. First, it has been indicated that M1 MP is an important initiator of angiogenesis. The inflammatory cytokines, such as TNF-α secreted by M1 MPs, have been demonstrated to induce an endothelial tip cell phenotype for sprouting[33] and are required for proper recovery of perfusion.[34] Inducible nitric oxide synthase has been proved to be proangiogenic,[35] and IL-1 has been found to be associated with the increased migration and proliferation of endothelial cells and ultimately organization into tubelike structures.[36] M1 MPs upregulated various genes involved in recruitment of endothelial cells, including vascular endothelial growth factor, fibroblast growth factor, and IL-8.[37] Also, the chemotactic factors released by M1 MPs, such as monocyte chemotactic protein 1, could enhance the collateral growth and perfusion.[38] Several studies have shown that local delivery of M1 MPs resulted in improvement in perfusion similar to that with treatment with M2 MPs.[14,15] Our results were in accordance with the clinical studies using BM-derived cells or granulocyte colony-stimulating factor-mobilized $CD34^+$ cells to improve perfusion.[16,39]

As noted previously, MPs are involved in skeletal muscle repair, and distinct MP populations are related to separate phases of muscle recovery.[6] It has been shown that LPS- and IFN-γ-

treated MPs altered their cytokine secretion on phagocytosis of necrotic debris and switched toward a proregenerative profile.[9] In vitro experiments have shown that M1 MPs promoted myoblast proliferation and decreased fibroblast collagen production.[9,40] Novak et al[41] revealed that exogenous M1 MPs reduced fibrosis and increased muscle regeneration after laceration injury. In accordance with these findings, we showed that M1 MPs accelerated clearance of necrotic tissue and increased IGF-1 expression in I/R injured muscle.[17] Data obtained from this study further demonstrated that M1 MPs hastened the regeneration process with elevated expression of MyoD at an early time point.

Notably, our previous study showed that injection of mature MPs at day 3 enhanced myofiber size and force production after I/R injury.[10] However, we did not observe the improved muscle force when delivering M2 MPs at day 1. It has been demonstrated that M2-inducing signals inhibit the expression of M1 chemokines[42]; hence, it is possible that delivering M2 MPs in the acute inflammatory phase interferes with regeneration, thereby impeding normal tissue formation. Further work will be required to verify this hypothesis and to elucidate how these two types of MPs coordinate in the course of regeneration. These results also indicate that the time point to inject MPs is critical to obtain the best therapeutic results.

CONCLUSIONS

In this investigation, we examined the transition of myeloid cells after ischemic injury and the effect of using exogenous MPs on restoration of perfusion and muscle function. Our data demonstrate that MPs not only participate in early tissue response but also improve perfusion and muscle regeneration and adaptation. These results provide insight into the potential use of in vitro polarized MPs in terms of the therapeutic delivery window and the magnitude of subsequent effects on angiogenesis and muscle healing after ischemic insult.

Supplementary Material

Refer to Web version on PubMed Central for supplementary material.

Acknowledgments

The authors would like to thank Dr Subhamoy Das for assistance with the speckle imaging.

REFERENCES

1. Weitz JI, Byrne J, Clagett GP, Farkouh ME, Porter JM, Sackett DL, et al. Diagnosis and treatment of chronic arterial insufficiency of the lower extremities: a critical review. Circulation 1996;94:3026–49. [PubMed: 8941154]
2. Hirsch AT, Criqui MH, Treat-Jacobson D, Regensteiner JG, Creager MA, Olin JW, et al. Peripheral arterial disease detection, awareness, and treatment in primary care. JAMA 2001;286:1317–24. [PubMed: 11560536]
3. McDermott MM, Greenland P, Liu K, Guralnik JM, Celic L, Criqui MH, et al. The ankle brachial index is associated with leg function and physical activity: the Walking and Leg Circulation Study. Ann Intern Med 2002;136:873–83. [PubMed: 12069561]

4. McDermott MM, Criqui MH, Greenland P, Guralnik JM, Liu K, Pearce WH, et al. Leg strength in peripheral arterial disease: associations with disease severity and lower-extremity performance. J Vasc Surg 2004;39:523–30. [PubMed: 14981443]
5. Tidball JG. Inflammatory cell response to acute muscle injury. Med Sci Sports Exerc 1995;27:1022–32. [PubMed: 7564969]
6. Tidball JG, Villalta SA. Regulatory interactions between muscle and the immune system during muscle regeneration. Am J Physiol Regul Integr Comp Physiol 2010;298: R1173–87. [PubMed: 20219869]
7. Nucera S, Biziato D, De Palma M. The interplay between macrophages and angiogenesis in development, tissue injury and regeneration. Int J Dev Biol 2011;55:495–503. [PubMed: 21732273]
8. Zordan P, Rigamonti E, Freudenberg K, Conti V, Azzoni E, Rovere-Querini P, et al. Macrophages commit postnatal endothelium-derived progenitors to angiogenesis and restrict endothelial to mesenchymal transition during muscle regeneration. Cell Death Dis 2014;5:e1031. [PubMed: 24481445]
9. Arnold L, Henry A, Poron F, Baba-Amer Y, van Rooijen N, Plonquet A, et al. Inflammatory monocytes recruited after skeletal muscle injury switch into antiinflammatory macrophages to support myogenesis. J Exp Med 2007;204:1057–69. [PubMed: 17485518]
10. Hammers DW, Rybalko V, Merscham-Banda M, Hsieh PL, Suggs LJ, Farrar RP. Anti-inflammatory macrophages improve skeletal muscle recovery from ischemia-reperfusion. J Appl Physiol (1985) 2015;118:1067–74. [PubMed: 25678696]
11. Gordon S, Taylor PR. Monocyte and macrophage heterogeneity. Nat Rev Immunol 2005;5:953–64. [PubMed: 16322748]
12. Troidl C, Jung G, Troidl K, Hoffmann J, Mollmann H, Nef H, et al. The temporal and spatial distribution of macrophage subpopulations during arteriogenesis. Curr Vasc Pharmacol 2013;11:5–12. [PubMed: 23391417]
13. Kuwahara G, Nishinakamura H, Kojima D, Tashiro T, Kodama S. Vascular endothelial growth factor-C derived from $CD11b^{+}$ cells induces therapeutic improvements in a murine model of hind limb ischemia. J Vasc Surg 2013;57: 1090–9. [PubMed: 23219511]
14. Kuwahara G, Nishinakamura H, Kojima D, Tashiro T, Kodama S. GM-CSF treated F4/80+ BMCs improve murine hind limb ischemia similar to M-CSF differentiated macrophages. PLoS One 2014;9:e106987. [PubMed: 25202910]
15. Jetten N, Donners MM, Wagenaar A, Cleutjens JP, van Rooijen N, de Winther MP, et al. Local delivery of polarized macrophages improves reperfusion recovery in a mouse hind limb ischemia model. PLoS One 2013;8:e68811. [PubMed: 23894348]
16. Raval Z, Losordo DW. Cell therapy of peripheral arterial disease: from experimental findings to clinical trials. Circ Res 2013;112:1288–302. [PubMed: 23620237]
17. Rybalko V, Hsieh PL, Merscham-Banda M, Suggs LJ, Farrar RP. The development of macrophage-mediated cell therapy to improve skeletal muscle function after injury. PLoS One 2015;10:e0145550. [PubMed: 26717325]
18. Dunn AK. Laser speckle contrast imaging of cerebral blood flow. Ann Biomed Eng 2012;40:367–77. [PubMed: 22109805]
19. Voyvodic PL, Min D, Liu R, Williams E, Chitalia V, Dunn AK, et al. Loss of syndecan-1 induces a pro-inflammatory phenotype in endothelial cells with a dysregulated response to atheroprotective flow. J Biol Chem 2014;289: 9547–59. [PubMed: 24554698]
20. Rybalko VY, Pham CB, Hsieh PL, Hammers DW, Merscham-Banda M, Suggs LJ, et al. Controlled delivery of SDF-1α and IGF-1: $CXCR4^{+}$ cell recruitment and functional skeletal muscle recovery. Biomater Sci 2015;3:1475–86. [PubMed: 26247892]
21. Shireman PK, Contreras-Shannon V, Ochoa O, Karia BP, Michalek JE, McManus LM. MCP-1 deficiency causes altered inflammation with impaired skeletal muscle regeneration. J Leukoc Biol 2007;81:775–85. [PubMed: 17135576]
22. Contreras-Shannon V, Ochoa O, Reyes-Reyna SM, Sun D, Michalek JE, Kuziel WA, et al. Fat accumulation with altered inflammation and regeneration in skeletal muscle of $CCR2^{-/-}$ mice following ischemic injury. Am J Physiol Cell Physiol 2007;292:C953–67. [PubMed: 17020936]

23. Brenes RA, Jadlowiec CC, Bear M, Hashim P, Protack CD, Li X, et al. Toward a mouse model of hind limb ischemia to test therapeutic angiogenesis. J Vasc Surg 2012;56: 1669–79. [PubMed: 22836102]
24. Peng X, Wang J, Lassance-Soares RM, Najafi AH, Sood S, Aghili N, et al. Gender differences affect blood flow recovery in a mouse model of hindlimb ischemia. Am J Physiol Heart Circ Physiol 2011;300:H2027–34. [PubMed: 21398592]
25. Ryan TE, Schmidt CA, Green TD, Brown DA, Neufer PD, McClung JM. Mitochondrial regulation of the muscle microenvironment in critical limb ischemia. Front Physiol 2015;6:336. [PubMed: 26635622]
26. Pipinos II, Swanson SA, Zhu Z, Nella AA, Weiss DJ, Gutti TL, et al. Chronically ischemic mouse skeletal muscle exhibits myopathy in association with mitochondrial dysfunction and oxidative damage. Am J Physiol Regul Integr Comp Physiol 2008;295:R290–6. [PubMed: 18480238]
27. Mann CJ, Perdiguero E, Kharraz Y, Aguilar S, Pessina P, Serrano AL, et al. Aberrant repair and fibrosis development in skeletal muscle. Skelet Muscle 2011;1:21. [PubMed: 21798099]
28. Martinez FO, Gordon S, Locati M, Mantovani A. Transcriptional profiling of the human monocyte-to-macrophage differentiation and polarization: new molecules and patterns of gene expression. J Immunol 2006;177:7303–11. [PubMed: 17082649]
29. Mantovani A, Sica A, Sozzani S, Allavena P, Vecchi A, Locati M. The chemokine system in diverse forms of macrophage activation and polarization. Trends Immunol 2004;25:677–86. [PubMed: 15530839]
30. Röszer T Understanding the mysterious M2 macrophage through activation markers and effector mechanisms. Mediators Inflamm 2015;2015:816460. [PubMed: 26089604]
31. Dziubek W, Bulińska K, Stefańska M, Wońniewski M, Kropielnicka K, Jasiński T, et al. Peripheral arterial disease decreases muscle torque and functional walking capacity in elderly. Maturitas 2015;81:480–6. [PubMed: 26119244]
32. Lemos DR, Babaeijandaghi F, Low M, Chang CK, Lee ST, Fiore D, et al. Nilotinib reduces muscle fibrosis in chronic muscle injury by promoting TNF-mediated apoptosis of fibro/adipogenic progenitors. Nat Med 2015;21:786–94. [PubMed: 26053624]
33. Sainson RC, Johnston DA, Chu HC, Holderfield MT, Nakatsu MN, Crampton SP, et al. TNF primes endothelial cells for angiogenic sprouting by inducing a tip cell phenotype. Blood 2008;111:4997–5007. [PubMed: 18337563]
34. Hoefer IE, van Royen N, Rectenwald JE, Bray EJ, Abouhamze Z, Moldawer LL, et al. Direct evidence for tumor necrosis factor-α signaling in arteriogenesis. Circulation 2002;105:1639–41. [PubMed: 11940540]
35. Kane AJ, Barker JE, Mitchell GM, Theile DR, Romero R, Messina A, et al. Inducible nitric oxide synthase (iNOS) activity promotes ischaemic skin flap survival. Br J Pharmacol 2001;132:1631–8. [PubMed: 11309233]
36. Voronov E, Carmi Y, Apte RN. The role IL-1 in tumor-mediated angiogenesis. Front Physiol 2014;5:114. [PubMed: 24734023]
37. Spiller KL, Anfang RR, Spiller KJ, Ng J, Nakazawa KR, Daulton JW, et al. The role of macrophage phenotype in vascularization of tissue engineering scaffolds. Biomaterials 2014;35:4477–88. [PubMed: 24589361]
38. Ito WD, Arras M, Winkler B, Scholz D, Schaper J, Schaper W. Monocyte chemotactic protein-1 increases collateral and peripheral conductance after femoral artery occlusion. Circ Res 1997;80:829–37. [PubMed: 9168785]
39. Kawamoto A, Katayama M, Handa N, Kinoshita M, Takano H, Horii M, et al. Intramuscular transplantation of G-CSF-mobilized $CD34^+$ cells in patients with critical limb ischemia: a phase I/IIa, multicenter, single-blinded, dose-escalation clinical trial. Stem Cells 2009;27: 2857–64. [PubMed: 19711453]
40. Song E, Ouyang N, Hörbelt M, Antus B, Wang M, Exton MS. Influence of alternatively and classically activated macrophages on fibrogenic activities of human fibroblasts. Cell Immunol 2000;204:19–28. [PubMed: 11006014]
41. Novak ML, Weinheimer-Haus EM, Koh TJ. Macrophage activation and skeletal muscle healing following traumatic injury. J Pathol 2014;232:344–55. [PubMed: 24255005]

42. Xiao T, Kagami S, Saeki H, Sugaya M, Kakinuma T, Fujita H, et al. Both IL-4 and IL-13 inhibit the TNF-α and IFN-γ enhanced MDC production in a human keratinocyte cell line, HaCaT cells. J Dermatol Sci 2003;31:111–7. [PubMed: 12670721]

ARTICLE HIGHLIGHTS

- **Type of Research:** In vivo experimental study of murine hind limb ischemia with macrophage-based cell therapy.
- **Take Home Message:** Evaluation of muscle damage and recovery with injection of proinflammatory and anti-inflammatory macrophages (MPs) into ischemic muscle revealed that exogenous administration of proinflammatory MPs improved recovery, muscle function, and size of fibers, whereas the anti-inflammatory MPs were associated with increased fibrosis.
- **Recommendation:** This study suggests that delivery of proinflammatory MPs in a temporally coordinated manner may be beneficial for ischemic muscle recovery in terms of muscle strength and blood supply.

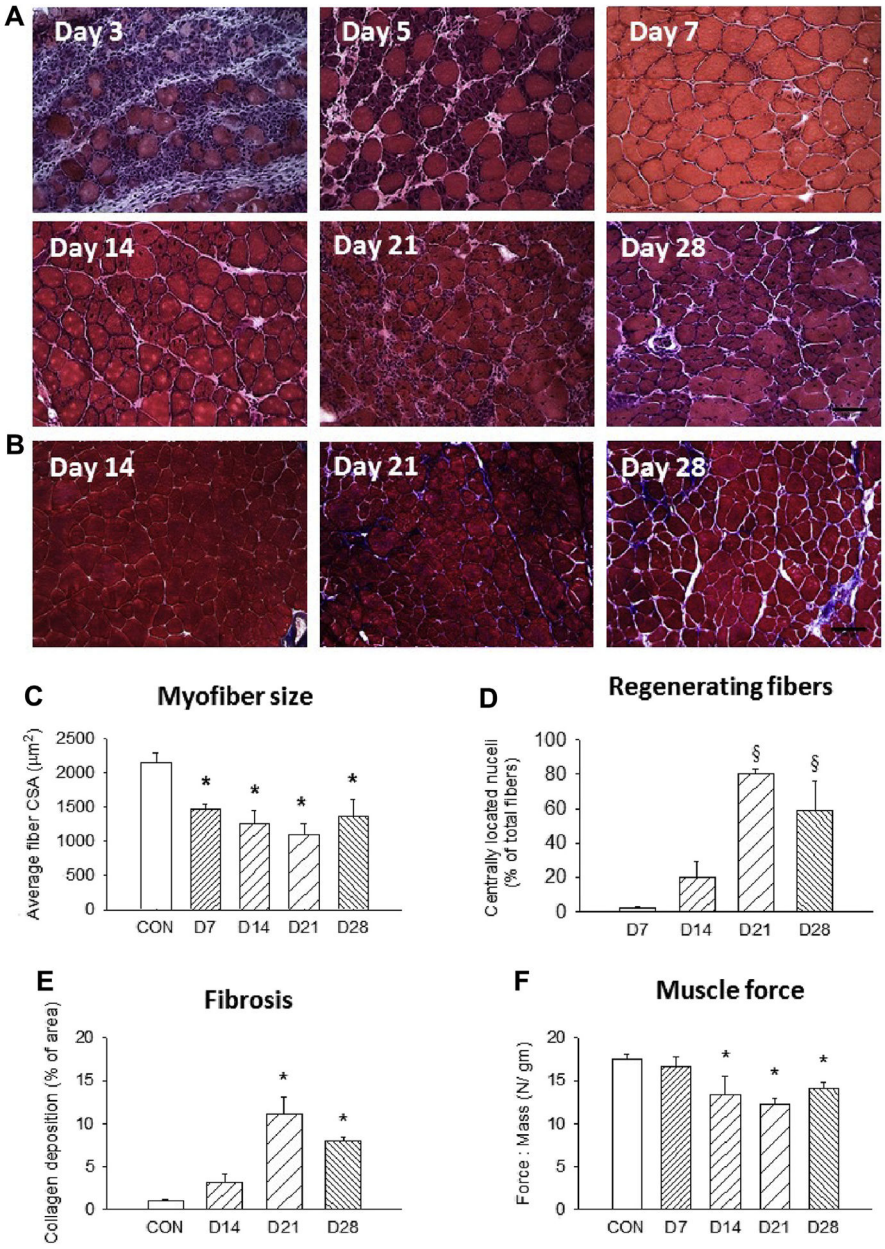

Fig 1.

Impaired muscle regeneration after femoral artery excision (FAE). Representative **(A)** hematoxylin and eosin and **(B)** trichrome staining images (20×) of FAE muscles at various time points. Quantification of **(C)** average myofiber size, **(D)** percentage of centrally nucleated myofibers, **(E)** area of collagen deposition, and **(F)** muscle force production. n = 5–7 for each time point; three fields of view/animal. *CON*, Contralateral side; *CSA*, cross-sectional area. *Scale bar* = 100 μm. Values are expressed as mean ± standard error of the mean; $^{*}P < .05$ compared with contralateral side; $^{\S}P < .05$ compared with day 7 group using one-way analysis of variance with post hoc Tukey honest significant difference.

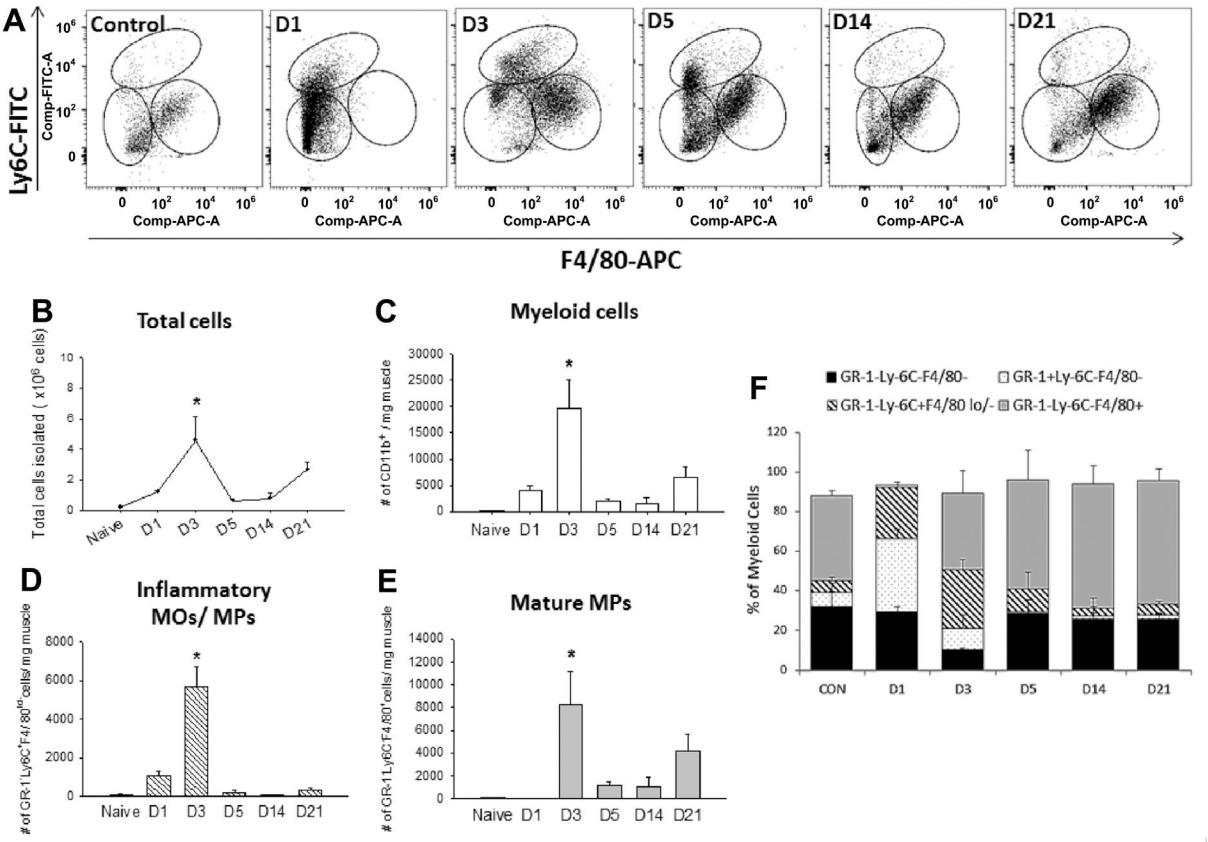

Fig 2.

Flow cytometry analysis of the myeloid cells in the ischemic muscles. **A**, After gating for $CD11b^+$ myeloid cells, three distinct subpopulations were evident on the basis of the expression of GR-1, Ly-6C, and F4/80, including $GR\text{-}1^+Ly\text{-}6C^-F4/80^-$ (neutrophils), $GR\text{-}1^-Ly\text{-}6C^+F4/80^{lo/-}$ (inflammatory monocytes [MOs]-macrophages [MPs]), and $GR\text{-}1^-Ly\text{-}6C^-F4/80^+$ (mature MPs). The temporal transition of myeloid cells shifted from $GR\text{-}1^+Ly\text{-}6C^-F4/80^-$ cells toward $GR\text{-}1^-Ly\text{-}6C^-F4/80^+$ cells. **B**, Total cell numbers peaked at day 3 after femoral artery excision (FAE) and increased again at day 21. Quantification of individual cell populations (cells per milligram of muscle), including **(C)** myeloid cells, **(D)** inflammatory MOs/MPs, and **(E)** mature MPs from day 1 to day 21. **F**, Percentage of each cell population in myeloid cells. Values are expressed as mean ± standard error of the mean; $*P < .05$ compared with naive muscles using one-way analysis of variance with post hoc Tukey honest significant difference. n = 3 for each time point. *APC*, Allophycocyanin; *CON*, contralateral side; *FITC*, fluorescein isothiocyanate.

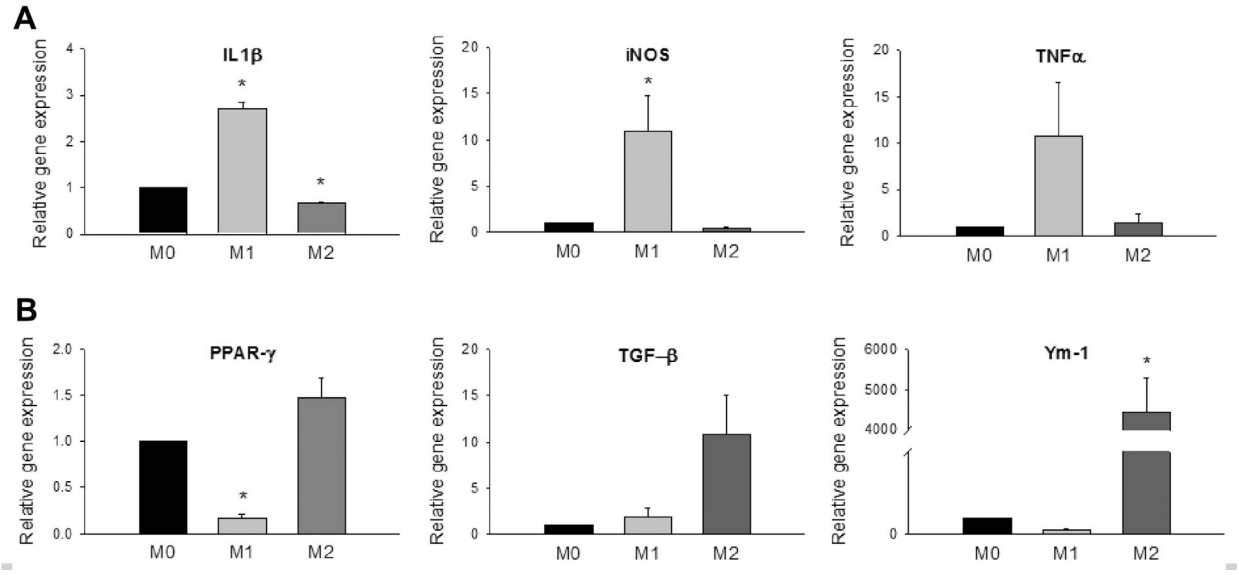

Fig 3.

In vitro polarized bone marrow (BM)-derived macrophages (MPs). After incubation of MP colony-stimulating factor for 5 days, BM-derived MPs were treated with either lipopolysaccharide (LPS) and interferon-γ (IFN-γ) to induce classical (*M1*) activation phenotype or interleukin 4 (IL-4) and IL-13 for alternative (*M2*) phenotypes. The untreated cells were designated *M0*. Real-time polymerase chain reaction (PCR) was performed to evaluate **(A)** inflammatory (interleukin 1β [*IL-1β*], inducible nitric oxide synthase [*iNOS*], tumor necrosis factor [*TNF-α*]) and **(B)** anti-inflammatory (peroxisome proliferator-activated receptor γ [*PPAR-γ*], transforming growth factor β1 [*TGF-β1*], Ym-1) gene expression. β-Actin was used as housekeeping gene. Values were expressed as mean ± standard error of the mean. **P* < .05 compared with M0 using one-way analysis of variance with post hoc Tukey honest significant difference.

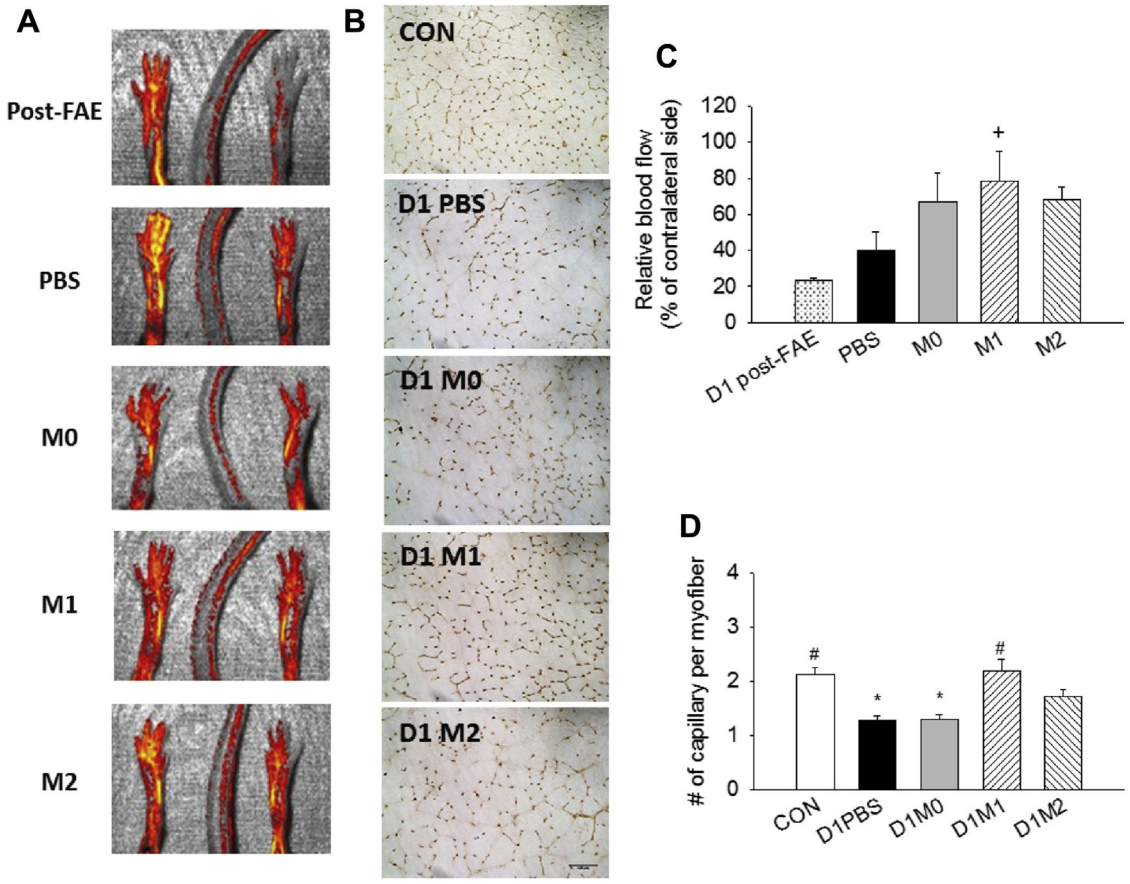

Fig 4.

Recovery of blood flow in ischemic limb after treatment with macrophages (MPs). **(A)** Representative images and **(C)** quantification of laser speckle for reperfusion at day 1 after femoral artery excision (*FAE*) and day 21 after FAE for each treatment group, including phosphate-buffered saline (*PBS*) and M0, M1, and M2 MPs. **(B)** Representative images (20×) and **(D)** quantification of $CD31^+$ endothelial cells for capillary-fiber ratio in day 21 post-FAE muscles. *CON*, Contralateral side. *Scale bar*: 100 μm. Values are expressed as mean ± standard error of the mean; $^+P < .05$ compared with D1 post-FAE using one-way analysis of variance with post hoc Dunnett test; $*P < .05$ compared with contralateral side; $^\#P < .05$ compared with PBS group using one-way analysis of variance with post hoc Tukey honest significant difference.

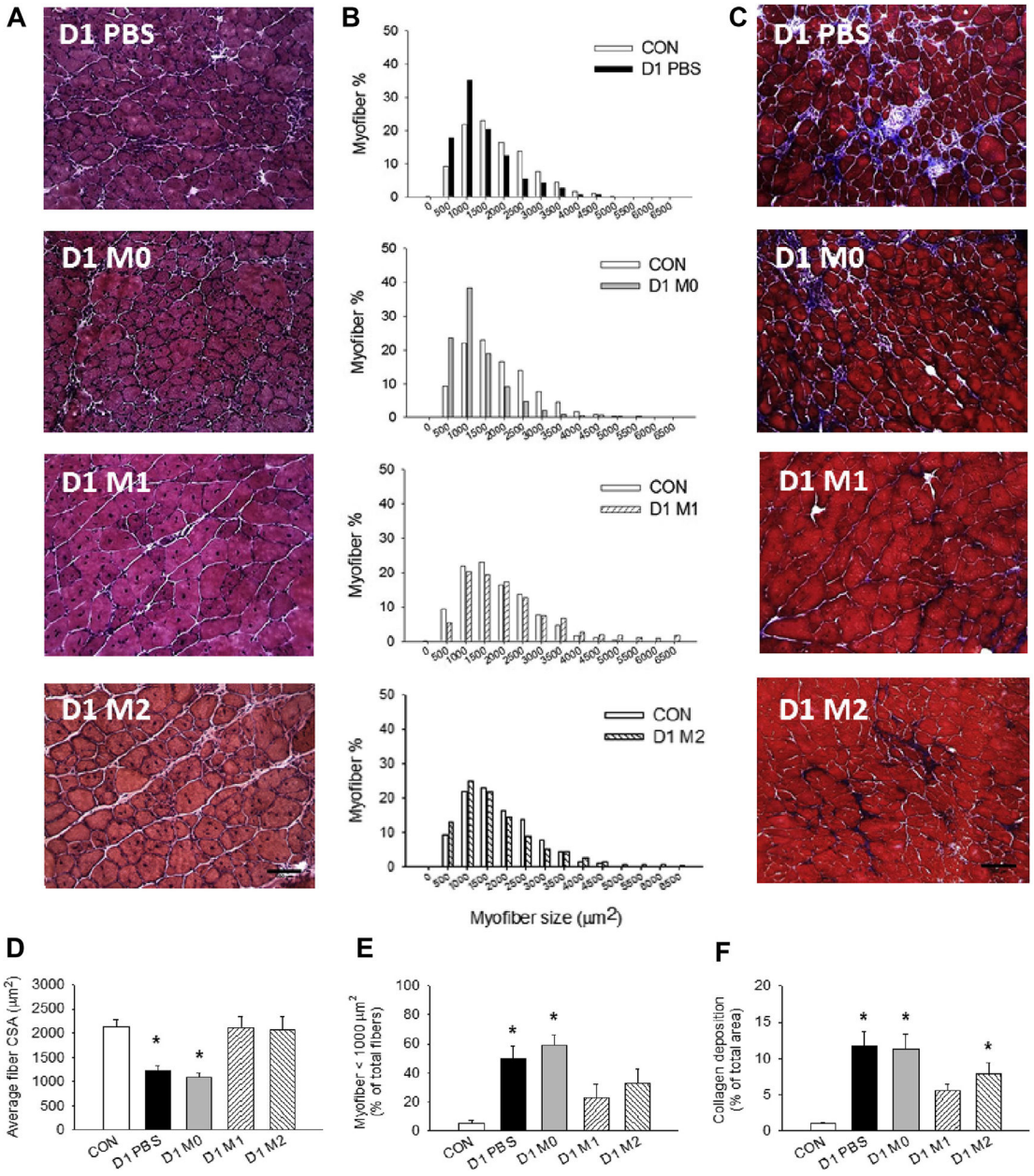

Fig 5.

Muscle repair after treatment with macrophages (MPs). Representative **(A)** hematoxylin and eosin and **(C)** trichrome staining images (20×) of ischemic muscles treated with phosphate-buffered saline (*PBS*) and M0, M1, or M2 MPs at day 21 after femoral artery excision (FAE). **B**, Myofiber size distribution relative to contralateral side. Quantification of **(D)** average myofiber size, **(E)** percentage of smaller myofibers, and **(F)** area of collagen deposition. n = 5–6 for each time point; three fields of view/animal. *CON*, Contralateral side; *CSA*, cross-sectional area. *Scale bar* = 100 μm. Values are expressed as mean ± standard error of the mean; **P* < .05 compared with contralateral side using one-way analysis of variance with post hoc Tukey honest significant difference.

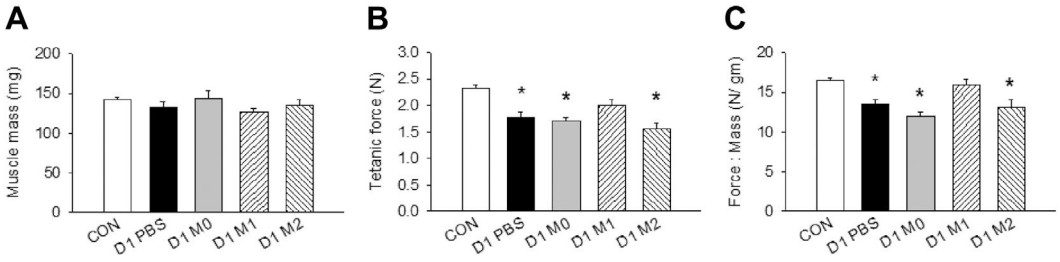

Fig 6.

Functional assessment of the ischemic muscles. **A**, Muscle mass. **B**, Tetanic force production of calf muscles. **C**, Normalized muscle force to muscle mass. *CON*, Contralateral side; *PBS*, phosphate-buffered saline. n = 5–6 for each group. Values are expressed as mean ± standard error of the mean; $*P < .05$ compared with contralateral side using one-way analysis of variance with post hoc Tukey honest significant difference.

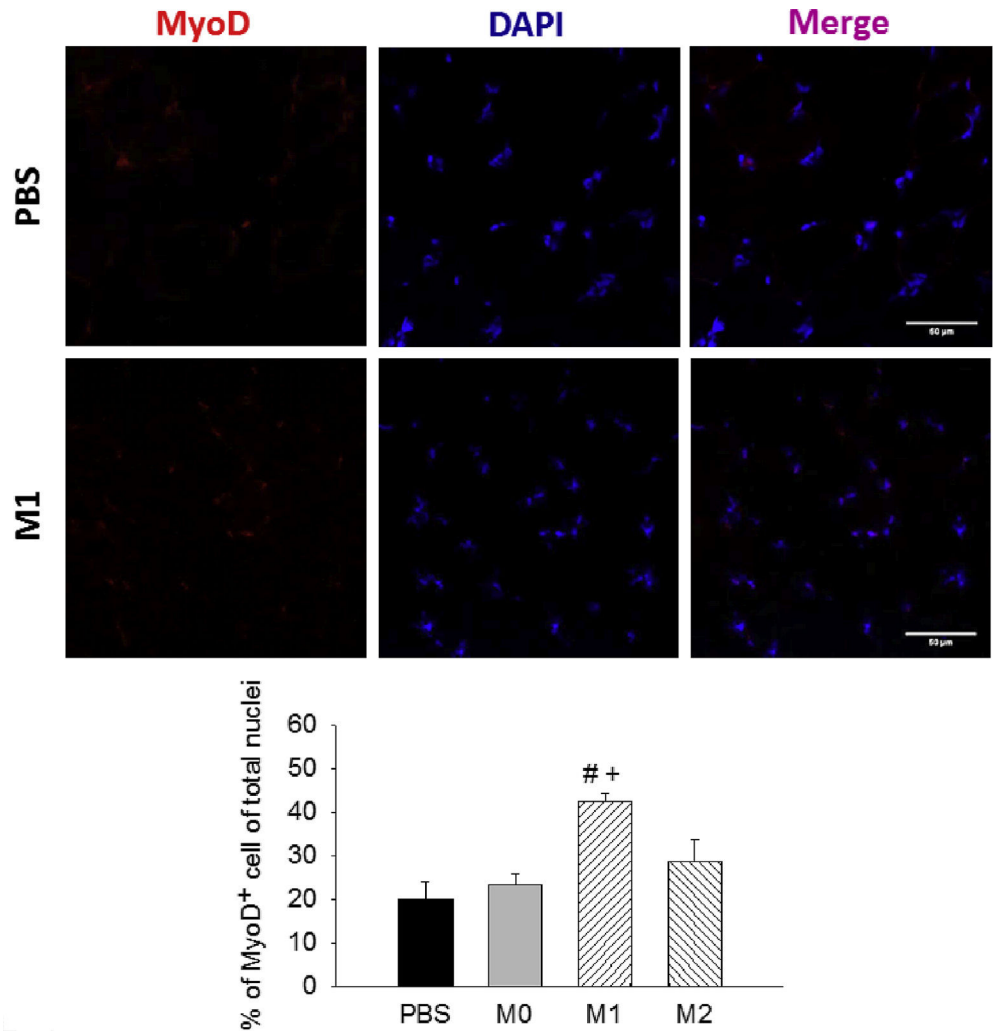

Fig 7.

MyoD staining in ischemic muscles at day 4 after femoral artery excision (FAE). Representative images (40×) of MyoD^{+} cells and quantification of MyoD-positive nuclei (% of total nuclei) among treatment groups. n = 3 for each group; five to seven images/animal. *DAPI*, 4′,6-Diamidino-2-phenylindole; *PBS*, phosphate-buffered saline. *Scale bar* = 50 μm. Values are expressed as mean ± standard error of the mean; $^{\#}P < .05$ compared with PBS group and $^{+}P < .05$ compared with M0 group using one-way analysis of variance with post hoc Tukey honest significant difference.

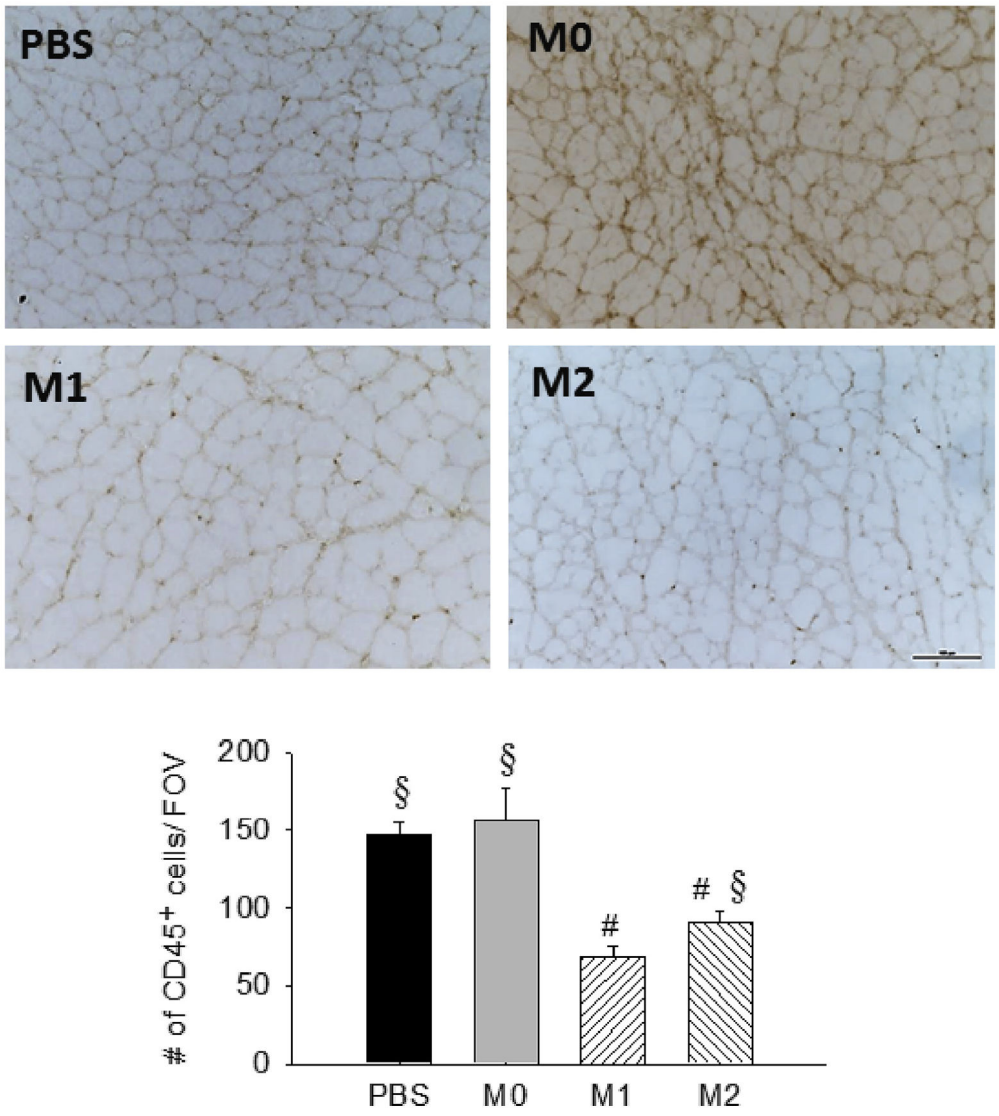

Fig 8.

Resolution of inflammation in ischemic muscles at day 21 after femoral artery excision (FAE). Representative images (20×) of $CD45^+$ cells and quantification of inflammatory cells per field of view (FOV) among treatment groups. n = 3–5 for each group; five images/animal. *PBS*, Phosphate-buffered saline. *Scale bar* = 100 μm. Values are expressed as mean ± standard error of the mean; $^{\#}P < .05$ compared with PBS group; $^{\S}P < .05$ compared with M1 group using one-way analysis of variance with post hoc Tukey honest significant difference.

Table.

Real-time polymerase chain reaction (PCR) primers

Gene	Forward (5′–3′)	Reverse (5′–3′)
Actb	AAGAGCTATGAGCTGCCTGA	TACGGATGTCAACGTCACAC
Nos2	TGACGGCAAACATGACTTCAG	GCCATCGGGCATCTGGTA
Tnfa	CCCACTCTGACCCCTTTACT	TTTGAGTCCTTGATGGTGGT
Il1b	CCCAACTGGTACATCAGCAC	TCTGCTCATTCACGAAAAGG
Tgfb	GCTACCATGCCAACTTCTGT	CGTAGTAGACGATGGGCAGT
PPARG	GCGGTGAACCACTGATATTC	TGTGGTAAAGGGCTTGATGT